On the use of line current analogues in geomagnetic depth sounding *

Alan G. Jones

Lithospheric Geophysics, Geological Survey of Canada, 1 Observatory Crescent, Ottawa, Ontario, Canada, K1A 0Y3

Abstract. Various workers have appealed to Biot-Savart's law for interpreting their anomalous geomagnetic response functions as an aid to describing the electromagnetic induction process. This approach, of using such a line current analogue, is shown herein to be erroneous if the conductivity of the lower half-space is not taken into consideration. A numerical solution, using an FFT, is derived from the kernels of the electromagnetic field components involved, and is compared with the simplistic solution offered by Biot-Savart's static field approximation. It is shown that within a close proximity of the surface position of the buried line current, Biot-Savart's law is reasonable. However, outwith this distance the *anomalous* magnetic field components, and accordingly their ratio, cannot be described by Biot-Savart's law, but closely resemble induction, at the inductive limit, in an isolated well-conducting inhomogeneity.

Uses of a line current in a conducting half-space as a suitable analogue of the true induction processes are illustrated with comparison to three anomalies – a conducting block, Alert, and the Great Glen fault.

Key words: Line current analogue – Electromagnetic induction – Alert – Great Glen fault

Introduction

In the field of electromagnetic induction studies of the Earth, many workers have found cause to interpret their observations in terms of a line (or sheet or box) current flowing beneath their recording locations as a convenient analogue for the actual induction processes that are taking place. Recently this approach has been used by Niblett et al. (1974), Wilhjelm and Friis-Christensen (1974), Alabi et al. (1975), Jankowski et al. (1977), Lilley and Woods (1978), Lienert (1979), Woods and Lilley (1980), DeLaurier et al. (1981), Lilley et al. (1981), Praus et al. (1981), Kirkwood et al. (1981), Ingham and Hutton (1982), Ingham et al. (1983) and Bingham et al. (1985). However, all of these authors considered that their line current was flowing in free space and used the static-field approximation which leads to Biot-Savart's law. The effect due to the conductivity of the lower half-space was neglected. In this work, this parameter is

treated in full and it is shown that the electromagnetic field components may be derived by Fourier transforming their respective kernels in the *wavenumber-frequency* domain.

The erroneous conclusions that result from treating the lower half-space as having zero conductivity are detailed and three examples are considered to illustrate the advantages of using a line current in a conducting half-space as an analogue for the true electromagnetic induction processes involved.

Theory

As shown, for example, in Patra and Mallick (1980, pp. 85–87), for an infinite line source oriented along the x direction at location $y=0$ and depth d in the lower half-space (denoted as region 1, of conductivity σ_1, permeability μ_1, and permittivity ε_1) of a two-media problem (Fig. 1) in which the discontinuity between the media is along the $z=0$ plane (the upper half-space, region 2, has appropriate parameters σ_2, μ_2 and ε_2, respectively), only the $\Pi_x(\omega)$ electric Hertz vector potential exists. This vector potential satisfies the Helmholtz equation

$$\frac{\partial^2}{\partial z^2} \Pi_x(y, z, \omega) + \frac{\partial^2}{\partial y^2} \Pi_x(y, z, \omega) - k_n^2 \Pi_x(y, z, \omega) = 0 \qquad (1)$$

where k_n is the electromagnetic wave propagation constant for the medium of interest, given by

$$k_n^2 = \omega \mu_n (i \sigma_n - \omega \varepsilon_n). \qquad (2)$$

The vector potential in the lower half-space is given by

$$\Pi_x^1 = \Pi_0 + \int_{-\infty}^{\infty} A e^{-\eta_1 z} e^{-i v y} dv \qquad (3a)$$

where Π_0 is the source term (see Patra and Mallick, 1980, p. 86), and in the upper half-space by

$$\Pi_x^2 = \int_{-\infty}^{\infty} B e^{\eta_2 z} e^{-i v y} dv, \qquad (3b)$$

where $\eta_i^2 = v^2 + k_i^2$ (the usual root chosen for η_i such that the solutions for A and B lead to physical fields) and v is the wavenumber. From the electric vector potential, the electromagnetic field components that exist, namely E_x, H_y and H_z, can be derived by

57
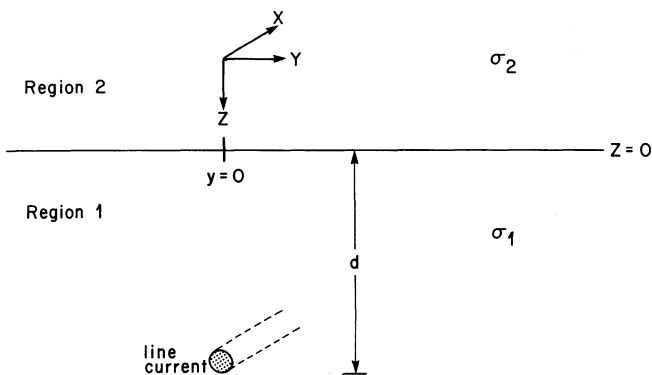
Fig. 1. The mathematical model to be considered. A line current, infinite in the x-direction, at y, z co-ordinates $(0, d)$ in the lower half-space (region 1) of a two half-space problem

$$E_x = -k^2 \Pi_x, \tag{4a}$$

$$H_y = \frac{k^2}{i\omega\mu} \frac{\partial \Pi_x}{\partial z} = \frac{-1}{i\omega\mu} \frac{\partial E_x}{\partial z}, \tag{4b}$$

$$H_z = -\frac{k^2}{i\omega\mu} \frac{\partial \Pi_x}{\partial y} = \frac{1}{i\omega\mu} \frac{\partial E_x}{\partial y}. \tag{4c}$$

The boundary conditions require that the tangential electric and magnetic field components are continuous across the $z = 0$ boundary. Hence, at $z = 0$

$$k_1^2 \Pi_x^1 = k_2^2 \Pi_x^2 \tag{5a}$$

from the continuity of E_x, and

$$k_1^2 \frac{\partial \Pi_x^1}{\partial z} = k_2^2 \frac{\partial \Pi_x^2}{\partial z} \tag{5b}$$

from H_y (assuming $\mu_1 = \mu_2$, and neither σ_1 nor σ_2 are infinite). Applying these boundary conditions at the interface $z = 0$ to Eq. (3b) leads to a solution for B such that the vector potential in the upper half-space is given by

$$\Pi_x^2(y, z, \omega) = I \frac{1}{2} \int_{-\infty}^{\infty} \left[\frac{i\omega\mu e^{-\eta_1 d}}{\pi k_2^2 (\eta_1 + \eta_2)} \right] e^{\eta_2 z} e^{-i v y} dv \tag{6}$$

(see Patra and Mallick, 1980, pp. 86–87) where I is the current flowing in the wire.

Just above the boundary $z = 0$, the three components of the electromagnetic fields present are given by Eq. (4),

$$E_x(y, 0, \omega) = I \frac{1}{2} \int_{-\infty}^{\infty} \left[\frac{-i\omega\mu}{\pi(\eta_1 + \eta_2)} e^{-\eta_1 d} \right] e^{-i v y} dv, \tag{7a}$$

$$H_y(y, 0, \omega) = I \frac{1}{2} \int_{-\infty}^{\infty} \left[\frac{-\eta_2}{\pi(\eta_1 + \eta_2)} e^{-\eta_1 d} \right] e^{-i v y} dv, \tag{7b}$$

$$H_z(y, 0, \omega) = I \frac{1}{2} \int_{-\infty}^{\infty} \left[\frac{i v}{\pi(\eta_1 + \eta_2)} e^{-\eta_1 d} \right] e^{-i v y} dv. \tag{7c}$$

Note that these integrals can be recognised as Fourier transformations from the wavenumber domain (v) into the space domain (y) of three kernel functions K_{E_x}, K_{H_y} and K_{H_z} given by

$$K_{E_x}(v) = \frac{-i\omega\mu}{\pi(\eta_1 + \eta_2)} e^{-\eta_1 d}, \tag{8a}$$

$$K_{H_y}(v) = \frac{-\eta_2}{\pi(\eta_1 + \eta_2)} e^{-\eta_1 d}, \tag{8b}$$

$$K_{H_z}(v) = \frac{i v}{\pi(\eta_1 + \eta_2)} e^{-\eta_1 d}. \tag{8c}$$

These kernels are such that $K_{E_x}(v)$ and $K_{H_y}(v)$ are symmetric, and $K_{H_z}(v)$ anti-symmetric, about $v = 0$.

The authors cited in the introduction all considered that their line currents were flowing in free space of zero conductivity. Accordingly, we may derive the electromagnetic field components observable by taking the appropriate values for their respective physical parameters for both region 1 and region 2, i.e. $\sigma_1 = \sigma_2 = 0$, $\varepsilon_1 = \varepsilon_2 = \varepsilon_0$, $\eta_1 = \eta_2 = \eta_0 = \sqrt{v^2 + k_0^2}$, $k_1 = k_2 = k_0 = \sqrt{(-\omega^2 \mu_0 \varepsilon_0)}$. The fields can be expressed as modified Bessel functions, with certain limiting forms,

$$E_x(y, 0, \omega) = I \frac{1}{2} \int_{-\infty}^{\infty} \left[\frac{-i\omega\mu_0 e^{-\eta_0 d}}{2\pi\eta_0} \right] e^{-i v y} dv \tag{9a}$$

$$= I \frac{-i\omega\mu_0}{2\pi} K_0(k_0 \sqrt{y^2 + d^2}) \tag{9b}$$

$$\approx I \frac{i\omega\mu_0}{2\pi} \ln(k_0 \sqrt{y^2 + d^2}) \tag{9c}$$

where the approximation is valid for $|k_0 \sqrt{y^2 + d^2}| \ll 1$ (Abramowitz and Stegun, 1970, 9.6.8),

$$H_y(y, 0, \omega) = I \frac{1}{2} \int_{-\infty}^{\infty} \left[\frac{-e^{-\eta_0 d}}{2\pi} \right] e^{-i v y} dv \tag{10a}$$

$$= \frac{I}{2\pi} \frac{k_0 d}{\sqrt{y^2 + d^2}} K_1(k_0 \sqrt{y^2 + d^2}) \tag{10b}$$

$$\approx \frac{I}{2\pi} \frac{d}{y^2 + d^2} \tag{10c}$$

and

$$H_z(y, 0, \omega) = I \frac{1}{2} \int_{-\infty}^{\infty} \left[\frac{i v e^{-\eta_0 d}}{2\pi\eta_0} \right] e^{-i v y} dv \tag{11a}$$

$$= \frac{I}{2\pi} \frac{k_0 y}{\sqrt{y^2 + d^2}} K_1(k_0 \sqrt{y^2 + d^2}) \tag{11b}$$

$$\approx \frac{I}{2\pi} \frac{y}{y^2 + d^2} \tag{11c}$$

where approximations (10c) and (11c) are valid for $|k_0 \sqrt{y^2 + d^2}| \ll 1$ (Abramovitz and Stegun, 1970, 9.6.9). Noting that the correct value of k_0 in free space is $k_0 = \sqrt{\omega\mu(i\sigma_0 - \omega\varepsilon_0)}$, and for values of ω of interest in electromagnetic induction studies ($< 10^5$ s^{-1}) neglecting σ_0 (valid for $\omega\varepsilon_0 \gg \sigma_0$, and $\sigma_0 \approx 10^{-13}$ S/m, Dolezalek, 1984) $k_0 \approx i\omega/c$, then this condition becomes $\omega \sqrt{y^2 + d^2} \ll c$. The static-field approximations given by Eqs. (10c) and (11c) can be recognised as Biot-Savart's law.

The forms (10c) and (11c) are those that have been utilised by the authors cited at the beginning of this note. Obviously, the ratio of the vertical magnetic field to the horizontal magnetic field, where both are due to a line current, is given by dividing Eq. (10b) by (11b)

58

$$\frac{H_z(y, 0, \omega)}{H_y(y, 0, \omega)} = \frac{y}{d}$$

when both regions 1 and 2 are considered to be free space. Also of significance is that the phase lead of E_x over H_y is $\pi/2$, i.e. they are totally out-of-phase, and the phase between H_z and H_y is 0, i.e. they are totally in phase.

However, for $\sigma_1 \neq 0$ and $\sigma_2 = 0$, as is the case for an infinite-length line current flowing at some depth d within a homogeneous half-space, then solutions to Eq. (7) must be sought. Closed-form solutions of these integrals do not appear to exist, and accordingly solutions must be sought resorting to numerical techniques taking advantage of the Fourier transform property of the three field-component kernels [Eq. (8)].

Discussion

To determine the validity of assuming that the line current is flowing in free space rather than within the lower half-space, it is of interest to examine the kernels [Eq. (8)] of the integrals. With medium 2 being free space, then $|\eta_2|$ $= \sqrt{|v^2 + k_2^2|} \approx \sqrt{v^2 - \omega^2/c^2} \approx |v|$ for $|v| \gg \omega/c$. Accordingly, for $|v| \gg \omega/c$, the kernels become

$$K_{E_x}(v) = \frac{-i\omega\mu}{\pi(\eta_1 + |v|)} e^{-\eta_1 d}, \tag{12a}$$

$$K_{H_y}(v) = \frac{-|v|}{\pi(\eta_1 + |v|)} e^{-\eta_1 d}, \tag{12b}$$

$$K_{H_z}(v) = \frac{iv}{\pi(\eta_1 + |v|)} e^{-\eta_1 d}. \tag{12c}$$

Note the interesting feature that the magnetic-field-component kernels given by Eq. (12b, c) are related by $K_{H_z}(v) = -i\,\mathrm{sgn}(v)\,K_{H_y}(v)$, which implies that $-H_z(y, 0, \omega)$ and $H_y(y, 0, \omega)$ form a Hilbert transform pair. Thus, for a dataset consisting of a profile of stations over a body whose response can be approximated by a line current analogue, the surface perpendicular-to-strike horizontal magnetic and vertical magnetic fields are related to each other by the Hilbert transform. This Hilbert transform relationship of internal anomalous fields has already been noted by Kertz (1954) (see also Berdichevsky and Zhdanov, 1984, pp. 200–201).

Obviously, the kernels given by Eq. (7) are only significantly different from the free space ones [Eqs. (9a), (10a), (11a)] when $|\eta_1| = \sqrt{(|v^2 + k_1^2|)} \gg |v|$, which is true for $|k_1|^2 = |\omega\mu(i\sigma_1 - \omega\varepsilon_1)| \gg |v|^2$. Assuming that the displacement-current term may be neglected in the conducting lower half-space, then this condition becomes $\omega\mu\sigma_1 \gg |v|^2$, i.e. for small values of wavenumber compared to the wave propagation constant in the conducting half-space. Note also that the free space kernels have dramatically different values at both zero and ω/c wavenumbers to those expressed by Eq. (12). For $v = 0$, then obviously $|\exp(-\eta_1 d)| \to 1$. For free space, $K_{E_x}(0) = -60\,\Omega$, $K_{H_y}(0) = -1/2\pi$ and $K_{H_z}(0) = 0$. However, for $\sigma_1 \neq 0$, then

$$K_{E_x}(0) \approx -i\omega\mu/\pi\sqrt{i\omega\mu\sigma_1} = -(1+i)\sqrt{\omega\mu/2\sigma_1}/\pi,$$

$$K_{H_y}(0) \approx -(1+i)\sqrt{\omega/\mu\sigma_1}/\pi c \quad \text{and} \quad K_{H_z}(0) = 0.$$

For $|v| = |k_0| = \omega/c$, then $\eta_0 = 0$, and in free space $K_{E_x}(|k_0|)$
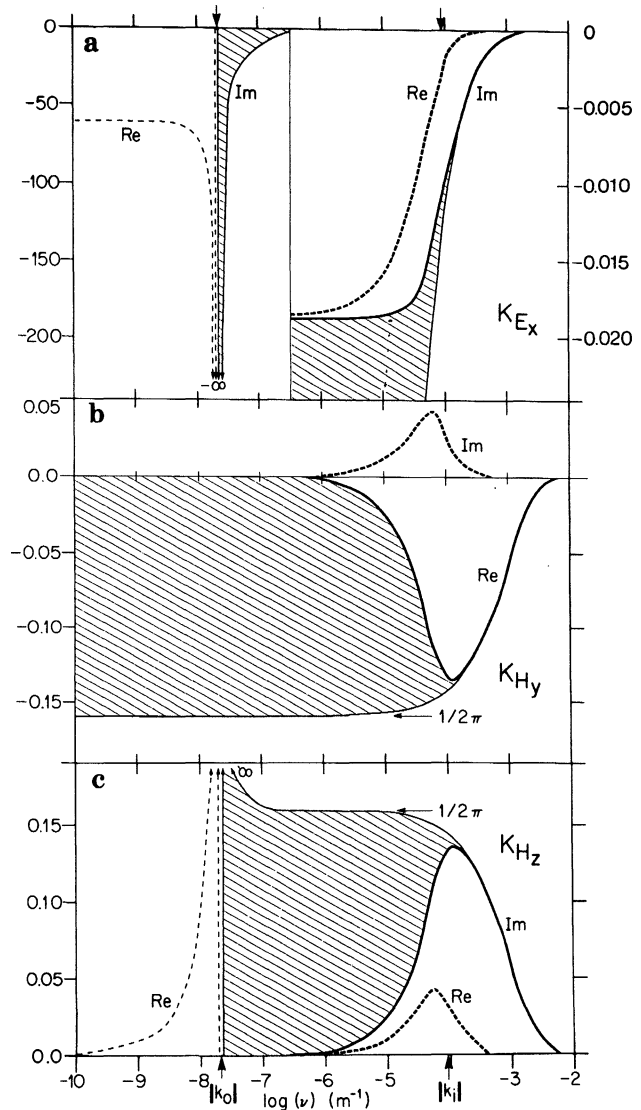
Fig. 2a–c. The bold lines illustrate the kernels for a line current at a depth of 1 km in a half-space of 1,000 Ωm excited at a frequency of 1 Hz, whereas the light lines are those for a line current in free space. The shaded regions are those areas included in the integral when the line current is considered to be in free space. a $K_{E_x}(v)$, (Im in full lines, Re in dashed) – note the dramatic change in ordinate scale at $v = 10|k_0|$, b $K_{H_y}(v)$, (Re in full lines, Im in dashed), c $K_{H_z}(v)$, (Im in full lines, Re in dashed)

$$= -(\infty + i\infty), \quad K_{H_y}(|k_0|) = 1/2\pi \quad \text{and} \quad K_{H_z}(|k_0|) = (\infty + i\infty);$$
whereas for a conducting lower half-space

$$K_{E_x}(|k_0|) \approx -(1+i)\sqrt{\omega\mu/2\sigma_1}/\pi,$$

$$K_{H_y}(|k_0|) = 0 \quad \text{and} \quad K_{H_z}(|k_0|) = (1+i)\sqrt{\omega/2\mu\sigma_1}/\pi c.$$

As an example, consider a half-space of $\sigma_1 = 10^{-3}$ S/m with a source line current at a depth of 1,000 m radiating with a frequency of 1 Hz. The kernels for such a configuration are illustrated in Fig. 2a–c. The contributions to the electromagnetic field components due to the conducting lower half-space are important for wavenumbers smaller than $\approx 10^{-6}$ m^{-1}. Note the dramatic difference at very small wavenumbers for K_{E_x} [there is a change of scale at $\log(v) = -6.5$] in Fig. 2a. The shaded areas of the three figures indicate those parts of the integrals that are included
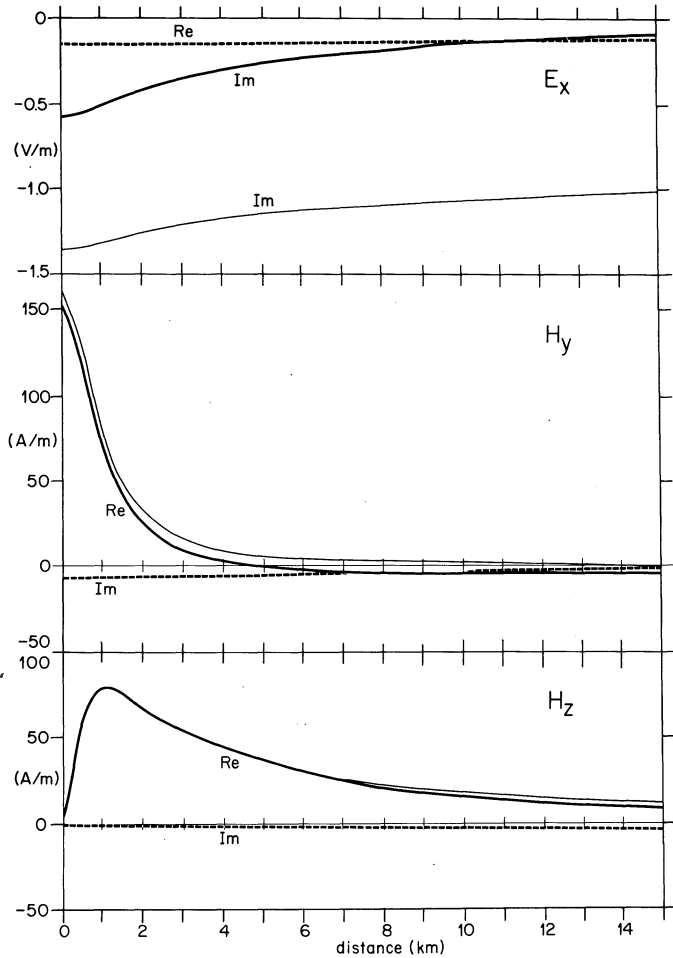
Fig. 3. The surface electromagnetic fields $E_x(y)$, $H_y(y)$, $H_z(y)$ given by a line current at a depth of 1 km in a half-space of 1,000 Ωm excited at a frequency of 1 Hz. The *light* lines are for the fields observed in a free space

Fig. 4. The ratio of the vertical magnetic field component to the horizontal magnetic field component for a line current at a depth of 1 km in a half-space of 1,000 Ωm excited at a frequency of 1 Hz. $\mathrm{Re}(H_z/H_y)$ denoted by *full* line, $\mathrm{Im}(H_z/H_y)$ as *dashed* line. The function y/d illustrates the response if the line current were considered to be in free space

when the conductivity of the lower half-space is not taken into consideration. Obviously,

$$\eta_1 = \sqrt{v^2 + k_1^2} = v[1 + (k_1/v)^2]^{1/2} \approx v[1 + (k_1/v)^2/2]$$

for $v \gg |k_1|$, and thus $\exp(-\eta_1 d) \approx \exp(-vd)(1 - k_1^2 d/2v)$ for large v. At $v = 10|k_1|$, then

$$K_{H_y} = -|v|/2\pi(\eta_1 + v) \exp(-\eta_1 d)$$

$$\approx (-1/2\pi) \exp(-vd)(1 - k_1 d/20).$$

For our example, $|k_1| d \approx 0.1$, and accordingly the free space kernel given by Eq. (10a) equals the conducting half-space kernel to within 0.5% at $v = 10|k_1|$.

In Fig. 3 are illustrated the three fields for a source current of 10^6 A derived by Fast Fourier Transforms of the three kernels in the range $v = [-81.92|k_1|, 81.92|k_1|]$ ($= [-7.28, 7.28] \times 10^{-2}$ m^{-1}) with $\Delta v = |k_1|/100$ ($= 8.88 \times 10^{-6}$ m^{-1}), i.e. each series of 16,384 complex points. Also shown in the figure are the fields that would be observed for a line current in free space, i.e. determined from Eq. (9c), (10c) and (11c). Ignoring the fact that the imaginary components of the magnetic fields cannot be computed for the free space formalism, $H_z(y, 0, \omega)$ is well-approximated by Biot-Savart's law out to a distance of

≈ 7 km. For $H_y(y, 0, \omega)$, the relative difference becomes significantly large at distances greater than ≈ 1 km, and indeed $\mathrm{Re}(H_y)$ changes sign at ≈ 5 km. This infers that the return currents are flowing beyond 5 km, whereas they flow at infinity for a line current in free space. It is apparent from the figure that $E_x(y, 0, \omega)$ is most affected by having a non-zero conductivity for the lower half-space. This is to be expected considering the greater attenuation of the electric field in a medium of non-zero conductivity. Accordingly, the anomalous electric field due to a line current source at depth within a conducting half-space is much smaller, for the same equivalent anomalous magnetic component magnitudes, than would arise if the current source were in free space. This feature implies that investigation of the possible effects on the computed magnetotelluric ratio of E_x^t/H_y^t (where superscript t denotes *total* fields) due to a line current source of the form carried out by, for example, Ingham and Hutton (1982), is of little practical use unless the conductivity of the host rock is taken into consideration. Ingham and Hutton quote an electric field magnitude due to a line current source of 3.5 mV/km; whereas in a half-space of 75 Ωm, a current of 127 A of 300 s periodicity at a depth of 50 km yields an electric field directly above the line of magnitude ≈ 0.1 mV/km. Note that in accordance with the requirement that $H_y(y)$ and $-H_z(y)$ form a Hilbert transform pair, $\mathrm{Re}(H_z)$ maximises approximately at the distance where $\mathrm{Re}(H_y)$ shows maximum gradient.

In induction studies, often the magnetic field components themselves are not as important as their ratios. The ratio H_z/H_y for free space is given simply by y/d. For the example described above, for which the fields are shown in Fig. 3, the ratio H_z/H_y is as illustrated in Fig. 4. As could be expected from the discussion above, y/d is a reasonable approximation out to ≈ 1 km. Accordingly, for stations within a "short" distance from the surface expression of the line current, where "short" here is obviously a function of the frequency of interest, the conductivity of the half-space and the depth of the line current, then the line current can be considered to be in free space. Beyond this distance, and out to ≈ 3 km, then a line current in free space at a depth of 750 m is a reasonable approximation to $\mathrm{Re}(H_z/H_y)$ (shown by the dashed line in Fig. 4). At distances greater than 3 km, then the response function cannot be

described by a line current in free space analogue. This is especially true at distances where the return currents flow, i.e. greater than 5 km, beyond which $\mathrm{Re}\,(H_y)$ has changed sign and accordingly $\mathrm{Re}\,(H_z/H_y)$ must change sign.

For a profile of *residual* magnetic observations, $H_y^r(y, 0, \omega)$ and $H_z^r(y, 0, \omega)$, i.e. observations of H_z and H_y that have had the effects of source fields, ocean effect, etc. removed, that are believed to originate from a channelled current that can be reasonably approximated by a line current, the most effective approach for modelling the data is to inverse Fourier transform the observations into the wavenumber-frequency domain, to give $H_y^r(v, 0, \omega)$ and $H_z^r(v, 0, \omega)$, and then find the best-fitting parameters I, σ_1 and d such that

$$H_y^r(v, 0, \omega) = I K_{H_y}(v)$$

and

$$H_z^r(v, 0, \omega) = I K_{H_z}(v)$$

are satisfied over all available frequencies ω. Interpretation in the wavenumber domain requires two Fourier transform operations (after suitable interpolating and extrapolating), and linear inverse theory can be applied directly to solve for the unknown parameters. In comparison, interpretation in the space domain requires two Fourier transform operations every time one (or more) of the parameters are changed.

Examples

In this section, I wish to consider three specific examples for which a line current in a conducting half-space provides a useful concept to describe the electromagnetic induction process.

Block

To compare the example chosen in the previous section to a model in which induction occurs, consider a square block of infinite length in the x-direction with sides 250 m long at a depth of 1 km in a host half-space of 1,000 Ωm (Fig. 5). The ratios of the vertical magnetic field to the *total* horizontal magnetic field (H_z/H_y^t) at 1 Hz for four different values of anomaly resistivity $(1 = 10\,\Omega\mathrm{m};\ 2 = 1\,\Omega\mathrm{m};\ 3 = 0.1\,\Omega\mathrm{m};\ 4 = 0.01\,\Omega\mathrm{m})$ are as illustrated in Fig. 6. By fitting a straight line to the initial rise of $\mathrm{Re}(H_z/H_y^t)$, one would conclude that the maximum depth of the anomaly, from y/d arguments, was at a depth of 20 km, 3.3 km, 1.67 km and 1.67 km for the four resistivities of the anomaly, respectively. Therefore, especially for anomalies of moderate resistivity contrast compared with the host rock, misleadingly deep maximum depths would be interpreted. However, if one considers the ratio of the vertical magnetic field component to the *anomalous* horizontal magnetic field component (H_z/H_y^a) – as illustrated in Fig. 7 – the initial rise of $\mathrm{Re}(H_z/H_y^a)$ would imply a maximum depth of ≈ 1.4 km (light *dashed* line in Fig. 7). Summers (1981) and Jones (1983) have previously suggested that H_z/H_y^a is a more useful response function to interpret for anomalous structure than is H_z/H_y^t. Jones (1983) defined "anomalous induction vectors" from the transfer functions relating $H_z(\omega)$ to $[H_x^a(\omega), H_y^a(\omega)]$. As is evident from Fig. 7, once the contrast in resistivity between the host rock and the anomaly reaches approximately three orders of magnitude (curve 2), then induc-
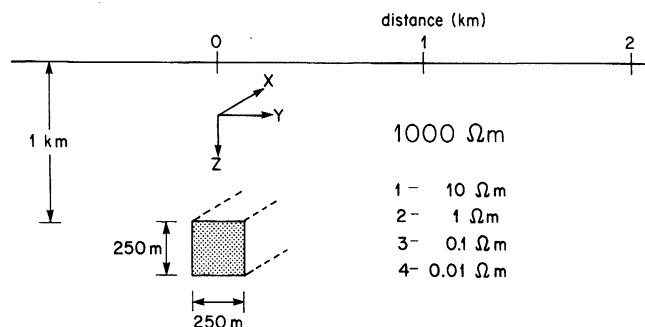

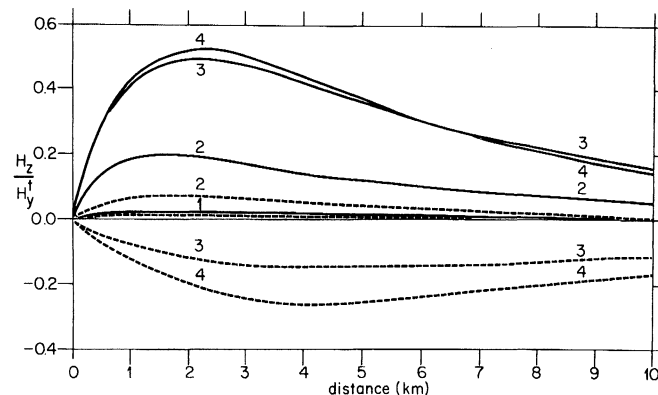**Fig. 5.** The block model discussed in the text

Fig. 6. The ratio of the vertical magnetic field to the *total* horizontal magnetic field, for the model illustrated in Fig. 5 at a frequency of 1 Hz for the four different block resistivities. $\mathrm{Re}[H_z(y)/H_y^t(y)]$ in *full* line, $\mathrm{Im}[H_z(y)/H_y^t(y)]$ *dashed* line
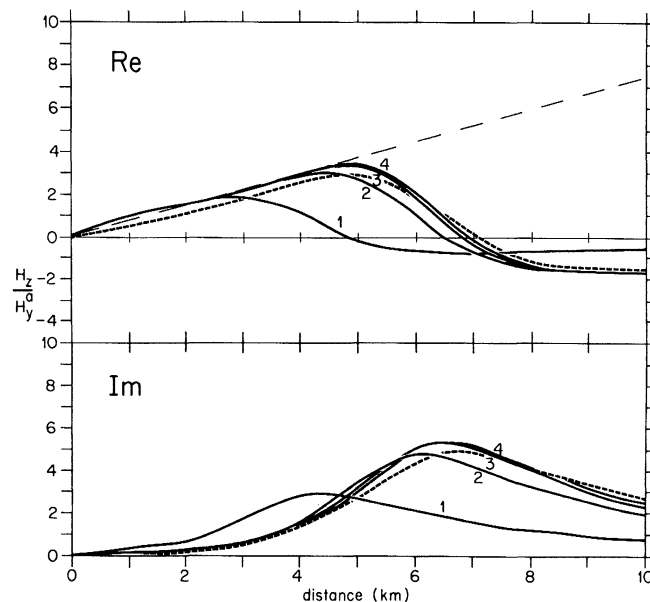

Fig. 7a, b. The ratio of the vertical magnetic field to the *anomalous* horizontal magnetic field, for the model illustrated in Fig. 5 at a frequency of 1 Hz for the four different block resistivities. **a** $\mathrm{Re}[H_z(y)/H_y^a(y)]$, **b** $\mathrm{Im}[H_z(y)/H_y^a(y)]$. The *light dashed* line in **a** is the y/d response for a line current in free space at a depth of 1.4 km and the *heavy dashed* lines in both **a** and **b** are the responses for a line current in a conducting half-space (of 1,000 Ωm) at a depth of 2 km
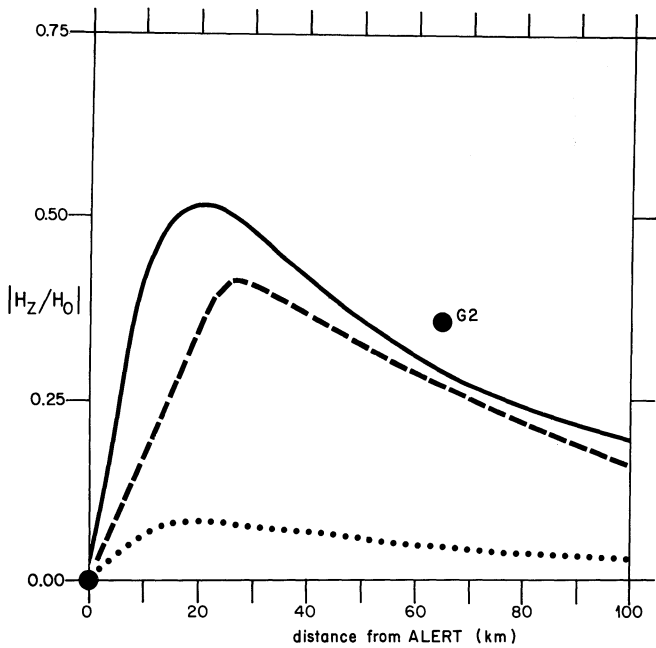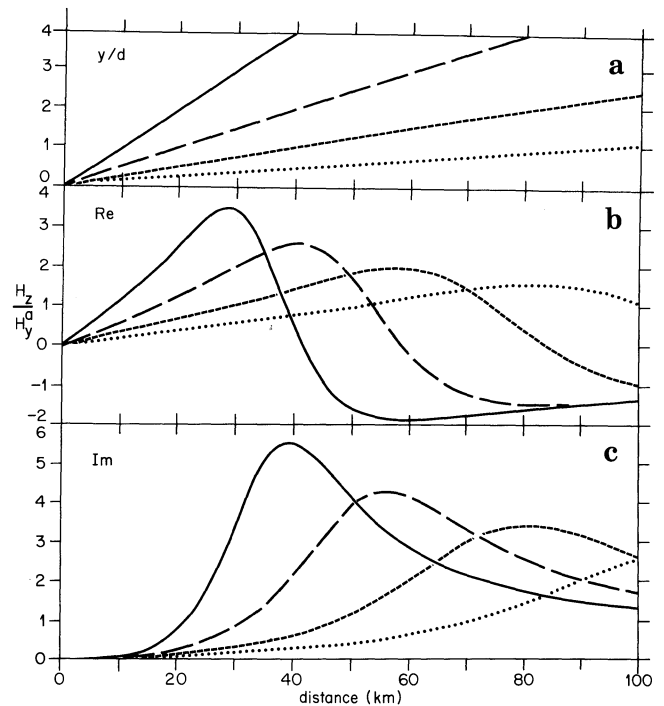
Fig. 8. The two *solid* dots indicate the ratio of $|H_z/H_0|$ observed at Alert and at station G2. The *dashed* line is the analogue response derived by Dyck and Garland for an embedded anomaly with its top at a depth of 25 km. The *dotted* line is the response for a line current in free space at 25 km, whilst the *full* line is the response for a line current in a half-space of 1,000 Ωm at a period of 2,000 s

Fig. 9a–c. Modelling the Great Glen fault using line currents. **a** The responses H_z/H_y to a line current in free space at depths of 10 km (*solid* line), 20 km (*long dashed* line), 40 km (*short dashed* line) and 80 km (*dotted* line). **b** and **c** are the responses when the line current is in a half-space of 100 Ωm for a period of 8 min

tion in the anomaly is at the inductive limit and the ratio of H_z/H_y^a does not change for greater contrast. However, the ratio of H_y^a/H_y^t varies with conductivity contrast and, accordingly, so does H_z/H_y^t (Fig. 6). Obviously, a line current in free space at a depth of 1.4 km (*light dashed* line in Fig. 7a) would well approximate $\mathrm{Re}(H_z/H_y^a)$ at distances out to ≈ 4–5 km, but not beyond that. However, a line current at a depth of 2 km in a conductive half-space of 1,000 Ωm, excited at 1 Hz (*heavy dashed* lines in Fig. 7a, b) is an excellent approximation to the response for both $\mathrm{Re}(H_z/H_y^a)$ and $\mathrm{Im}(H_z/H_y^a)$ over the whole distance range.

Alert

The Alert anomaly on Ellesmere Island in northern Canada was one of the first geological structures in the crust whose geomagnetic response was ascribed to current channelling rather than local induction. Figure 8 displays two of the $|H_z/H_0|$ ratios – where H_0 is the "normal" horizontal magnetic field as observed at a station some 120 km from Alert (Law et al., 1963) – for the Alert anomaly and for station G2 as published by Dyck and Garland (1969) and taken from Whitham (1964). The analogue response of an embedded anomaly with dimensional scaling such that it is equivalent to an anomaly 20 km deep, 30 km width and 15 km vertical extent with a conductivity contrast to the host rock of 7×10^4 at a period of 2,000 s was determined by Dyck and Garland and is shown here in Fig. 8 (*dashed* line). Also shown in the figure are the $|H_z/H_0|$ ratios for a line current in free space at 25 km depth (*dotted* line, note that this response is not simply y/d because we are normalizing H_z by the horizontal magnetic field at $y = 120$ km, and not by the local H_y) and a line current in a half-space of 10^4 Ωm at a depth of 25 km radiating at 2,000 s (*solid* line). It is

obvious that whereas the free space line current is not a good simplification, the line current in a conducting half-space is.

Great Glen fault

The geomagnetic anomaly associated with the Great Glen fault in northern Scotland was studied using a line current in free space analogue by Kirkwood et al. (1981). Figure 9a shows the H_z/H_y^a ratio as y/d for a line current in free space at 10 km (*solid* line), 20 km (*long dashed* line), 40 km (*short dashed* line) and 80 km (*dotted* line). Figure 9b and c display $\mathrm{Re}(H_z/H_y^a)$ and $\mathrm{Im}(H_z/H_y^a)$, respectively, for a line current in a half-space of resistivity 100 Ωm at the four depths given above. It is obvious that the initial rise of $\mathrm{Re}(H_z/H_y^a)$ is well-approximated by a line current in free space, i.e. out to distances of 25, 40, 60 and 85 km for depths of 10, 20, 40 and 80 km, although the depth estimates would be in error. However, beyond these distances, the full solution must be used for $\mathrm{Re}(H_z/H_y^a)$.

Conclusions

It has been shown unequivocally that when one is attempting to interpret observed responses due to induction in an anomaly by using a line current analogue, it is not sufficient to ignore the conductivity of the half-space in which the current is flowing. This is especially true at distances where the return currents are flowing.

Three examples have been chosen to illustrate that induction in a body may be described by a line current in a conducting half-space provided that the induction is at the "inductive limit". Also, the necessity for considering

the transfer function H_z/H_y^a, rather than H_z/H_y^t, has been stressed.

The Fast Fourier Transform calculations used herein are not particularly "fast" when compared to numerical modelling – only a factor of three increase in speed is realized – however, that was not the thrust of this work. For practical application of a fast line current approximation solution, then either linear filter methods can be used (Johansen and Sorensen, 1979) or Logarithmic Fourier Transforms (Talman, 1978).

References

Abramowitz, M., Stegun, I.A.: Handbook of Mathematical Functions. Dover, New York, 1970

Alabi, A.O., Camfield, P.A., Gough, D.I.: The North American Central Plains anomaly. Geophys. J.R. Astron. Soc. **43**, 815–834, 1975

Berdichevsky, M.N., Zhdanov, M.S.: Advanced theory of deep geomagnetic sounding. Elsevier, ISBN 0-444-41690-0, 1984

Bingham, D.K., Gough, D.I., Ingham, M.R.: Conductive structures under the Canadian Rocky Mountains. Can. J. Earth Sci. **22**, 384–398, 1985

DeLaurier, J.M., Plet, F.C., Drury, M.J.: A geomagnetic depth sounding profile across the northern Yukon and the Mackenzie Delta region, Canada. Can. J. Earth Sci. **18**, 1092–1100, 1981

Dolezalek, H.: Atmospheric electricity. In: CRC Handbook of chemistry and physics, 65th Edition, R.C. Weast, ed.: pp. F-158–F-160. Boca Raton, Florida: CRC Press Inc., 1984

Dyck, A.V., Garland, G.D.: A conductivity model of certain features of the Alert anomaly in geomagnetic variations. Can. J. Earth Sci. **6**, 513–516, 1969

Ingham, M.R., Bingham, D.K., Gough, D.I.: A magnetovariational study of a geothermal anomaly. Geophys. J.R. Astron. Soc. **72**, 597–618, 1983

Ingham, M.R., Hutton, V.R.S.: Crustal and upper mantle electrical conductivity structure in southern Scotland. Geophys. J.R. Astron. Soc. **68**, 579–594, 1982

Jankowski, J., Szymanski, A., Pec, K.: Electromagnetic studies of the Carpathian conduction anomaly. Acta Geodaet. Geophys. et Montanist. Acad. Sci. Hung. **12**, 99–109, 1977

Johansen, H.K., Sorensen, K.: Fast Hankel Transforms. Geophys. Prospect. **27**, 876–901, 1979

Jones, A.G.: The problem of "current channelling": a critical review. Geophys. Surv. **6**, 79–122, 1983

Kertz, W.: Modelle für erdmagnetischen induzierte elektrische Ströme in Untergrund. Nachr. Akad. Wiss. Göttingen, Math.-Phys. Kl. **11A**, 101–110, 1954

Kirkwood, S.C., Hutton, V.R.S., Sik, J.: A geomagnetic study of the Great Glen fault. Geophys. J.R. Astron. Soc. **66**, 481–490, 1981

Law, L.K., DeLaurier, J., Andersen, F., Whitham, K.: Investigations during 1962 of the Alert anomaly in geomagnetic variations. Can. J. Phys. **41**, 1868–1882, 1963

Lienert, B.R.: Crustal electrical conductivities along the eastern flank of the Sierra Nevadas. Geophysics **44**, 1830–1845, 1979

Lilley, F.E.M., Singh, B.P., Arora, B.R., Srivastava, B.J., Prasad, S.N., Sloane, M.N.: A magnetometer array study in northwest India. Phys. Earth Planet. Inter. **25**, 232–240, 1981

Lilley, F.E.M., Woods, D.V.: The channelling of natural electric currents by orebodies. Bull. Aust. Soc. Explor. Geophys. **9**, 62–63, 1978

Niblett, E.R., DeLaurier, J.M., Law, L.K., Plet, F.C.: Geomagnetic variation anomalies in the Canadian Arctic. I. Ellesmere island and Lincoln Sea. J. Geomagn. Geoelectr. **26**, 203–221, 1974

Patra, H.P., Mallick, K.: Geosounding principles, 2. Time-varying geoelectric soundings. Amsterdam: Elsevier, 1980

Praus, O., Pecova, J., Petr, V., Pec, K., Hvozdara, M., Cerv, V., Pek, J., Lastovickova, M.: Electromagnetic induction and electrical conductivity in the Earth's body. In: Geophysical synthesis in Czechoslovakia, A. Zátopek, ed.: pp. 297–315, Bratislava: Veda, 1981

Summers, D.M.: Interpreting the magnetic fields associated with two-dimensional induction anomalies. Geophys. J.R. Astron. Soc. **65**, 535–552, 1981

Talman, J.D.: Numerical Fourier and Bessel transforms in logarithmic variables. J. Comput. Phys. **29**, 35–48, 1978

Whitham, K.: Anomalies in geomagnetic variations in the Arctic Archipelago of Canada. J. Geomagn. Geoelectr. **15**, 227–240, 1964

Wilhjelm, J., Friis-Christensen, E.: The Igdlorssuit geomagnetic variation anomaly in the rift-fault zone of northern west Greenland. J. Geomagn. Geoelectr. **26**, 173–189, 1974

Woods, D.V., Lilley, F.E.M.: Anomalous geomagnetic variations and the concentration of telluric currents in south-west Queensland, Australia. Geophys. J.R. Astron. Soc. **62**, 675–689, 1980